Journal of Zhejiang University-SCIENCE B (Biomedicine & Biotechnology) *2021 22(9):774-781*
www.jzus.zju.edu.cn; www.springer.com/journal/11585
E-mail: jzus_b@zju.edu.cn

Correspondence

https://doi.org/10.1631/jzus.B2000793

Pulsed low-dose rate radiotherapy has an improved therapeutic effect on abdominal and pelvic malignancies

Xin WEN[2], Hui QIU[2], Zhiying SHAO[3], Guihong LIU[2], Nianli LIU[1], Aoxing CHEN[2], Xingying ZHANG[2], Xin DING[2]✉, Longzhen ZHANG[1,2,4]✉

[1]*Cancer Institute of Xuzhou Medical University, Xuzhou 221000, China*
[2]*Department of Radiation Oncology, Affiliated Hospital of Xuzhou Medical University, Xuzhou 221000, China*
[3]*Department of Interventional Ultrasound, Zhejiang Cancer Hospital, Hangzhou 310000, China*
[4]*Jiangsu Center for the Collaboration and Innovation of Cancer Biotherapy, Xuzhou 221000, China*

Until now, there has been a lack of standard and effective treatments for patients with recurrent malignant tumors or abdominal and pelvic malignancies with extensive invasion (Morris, 2000). Generally, these patients face problems such as inability to undergo surgery or chemotherapy resistance (Combs et al., 2016). Re-radiotherapy has achieved a prominent place in the treatment of patients who have received radiotherapy previously and developed in-field recurrences (Straube et al., 2018). However, re-radiotherapy is very complicated, requiring comprehensive consideration of appropriate radiation dose, interval from first radiotherapy, boundary of the radiotherapy target area, and damage to surrounding normal tissues (Straube et al., 2019). In other words, it is necessary to focus on the protection of surrounding normal tissues while maximizing the efficacy of re-radiotherapy in such patients.

Over the years, many studies have been done on the effect of dose rate in radiotherapy (Martin et al., 2013). According to the classical cell survival curve of hypersensitivity (Fig. 1a), hyper-radiosensitivity (HRS) is observed in cancer cells exposed to low-dose rate radiotherapy (<0.30 Gy), with a steeper slope of survival curve than that of high-dose rate radiotherapy. When the radiotherapy dose reaches 0.30–0.60 Gy, radiosensitivity begins to shift to increased radioresistance (IRR) (Todorovic et al., 2020). The HRS/IRR phenomenon can be defined using the induced repair model: $SF(d)=\exp\{-\alpha_r[1+(\alpha_s/\alpha_r-1)\exp(-d/d_c)]d-\beta d^2\}$, where SF is surviving fraction, d is radiation dose, α_r is the slope of survival curve of high-dose rate radiation, α_s is the slope of survival curve of low-dose rate radiation, d_c is the threshold of transition from HRS to IRR, and β indicates the indirect lethal effect of radiation on cells (Wang et al., 2017). Therefore, rapidly proliferating cancer cells should be more sensitive to low-dose rate radiotherapy than normal tissue cells with low or no proliferation. Moreover, d_c is different between cancers (d_c=0.30–0.50 Gy) and normal tissues (d_c<0.20 Gy) (Dai et al., 2009). That is to say, at low-dose rates, HRS occurred in tumors while over-repair effects occurred in normal tissues. On the radiobiological basis of HRS/IRR and sublethal injury repair (Fig. 1b) (Elkind et al., 1965), pulsed low-dose rate (PLDR) radiotherapy emerged as the times require.

The implementation strategy for PLDR involves dividing 2.00 Gy into ten fractions and administering each irradiating dose of 20 cGy at an interval of 3 min before the next low-dose radiation (Li et al., 2019). The pulse dose is within the dose range for tumor radiosensitivity and normal tissue radioresistance, which can contribute to a higher rate of tumor cell apoptosis while better protecting normal tissues from radiation damage. Relevant basic and clinical studies have shown that PLDR improves the local control

✉ Longzhen ZHANG, jsxyfyzlz@126.com
Xin DING, dingxin81@163.com
Longzhen ZHANG, https://orcid.org/0000-0002-5786-1560
Xin DING, https://orcid.org/0000-0001-6055-5292
Xin WEN, https://orcid.org/0000-0002-1649-3669
Hui QIU, https://orcid.org/0000-0002-5819-0965

Received Dec. 9, 2020; Revision accepted Apr. 13, 2021;
Crosschecked Aug. 26, 2021

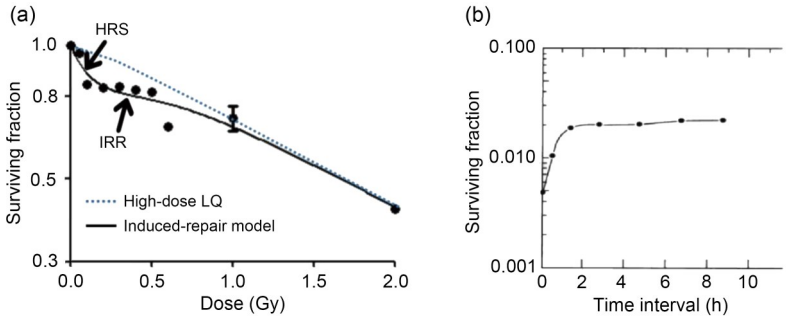

Fig. 1 Induced-repair model of PLDR. (a) Typical cell survival curve with evidence of HRS/IRR. Broken line shows low-dose extrapolation from linear quadratic model applied to high-dose survival data. Solid line shows induced repair fit. (b) The description of the sublethal repair half time of normal cells by Elkind et al. (1965). The hamster cells were irradiated with total 1558 cGy, which divided evenly into 763 cGy and 795 cGy with different intervals and cells were placed at room temperature during the interval. PLDR: pulsed low-dose rate; HRS: hyper-radiosensitivity; IRR: increased radioresistance; LQ: linear-quadratic model.

rate and the quality of life of cancer patients (Li et al., 2019).

Considering that the optimal pulse dose for different cancers is different (Pavlopoulou et al., 2017), it is important to study the optimal PLDR model for different types of tumors, especially abdominal and pelvic malignancies, so as to achieve effective treatment and make the PLDR technique accessible on a larger scale. Hence, we studied the optimal PLDR models for pancreatic cancer and prostate cancer.

We first investigated the HRS phenomenon in prostate cancer and pancreatic cancer by colony formation assay (Fig. 2a). Prostate cancer cells (PC3, 22Rv1, and DU145) and pancreatic cancer cells (PANC-1, BXPC-3, and CFPAC-1) were one-off irradiated with 0, 0.05, 0.10, 0.20, 0.30, 0.40, 0.50, 1.00, and 2.00 Gy, at a dose rate of 100 cGy/min. Our results (Table 1, Figs. 2b–2d, and Figs. 2f–2h) showed that after low-dose (<0.30 Gy) radiotherapy, the plating efficiencies (PEs) and SFs of cancer cells decreased rapidly; however, when the radiation dose was 0.30–1.00 Gy, the PEs and SFs did not decrease significantly, but slightly increased. The survival curves (Figs. 2e and 2i) showed the same trend, suggesting that prostate cancer cells and pancreatic cancer cells changed from HRS to IRR within the dose range of 0.30 to 1.00 Gy. Furthermore, according to the parameter values in the induced repair model shown in Table 1, we found that the α_s of each cancer cell was markedly higher than the α_r, indicating that the radiation sensitivity under low-dose conditions was significantly higher than that under conventional-dose conditions. These results indicated that all six cancer cell lines used in this study displayed the HRS/IRR phenomenon. We also found that both radiosensitive cells (such as BXPC-3, DU145, and CFPAC-1) and radioresistant cells (such as PANC-1) had HRS phenomena, suggesting that HRS/IRR was not unique to radioresistant cancer cells. Compared with other cancer cells, PANC-1 cells had the most evident radiation resistance, but not the most significant HRS phenomenon. Therefore, it is not the case that the more obvious the radiation resistance at the conventional dose, the more significant the HRS phenomenon at a low dose. In order to fully guarantee the radiation sensitivity of cancer cells, the pulse dose d in PLDR should be less than or equal to the transition dose d_c; in other words, the pulse dose d should be as close as possible to d_c. Based on the d_c of each cell shown in Table 1, we determined the pulse dose d of both pancreatic and prostate cancer cells to be 0.20 Gy.

Next, we studied the time interval in PLDR in terms of the sublethal repair half-time ($t_{1/2}$) of peripheral normal cells. According to previous study (Li et al., 2019), time interval in PLDR is calculated by the following formulae: $t=t_{1/2}/(m-1)$, $m=D/d$ (t is the time interval, $t_{1/2}$ is the sublethal repair half-time, D is radiation dose, d is pulse dose, and m is pulse number). The normal tissues around pancreatic cancer include pancreas, small intestine, and liver; the normal tissues around prostate cancer include prostate, rectum, and bladder. HRS mainly affects early-response tissues, while liver and bladder are late-response tissues with the radiobiologic ratio of lethal to sublethal damage (α/β) smaller than that of tumors; they are thus more likely to repair damage at low-dose radiation levels (Harney et al., 2004). Therefore, we did not consider

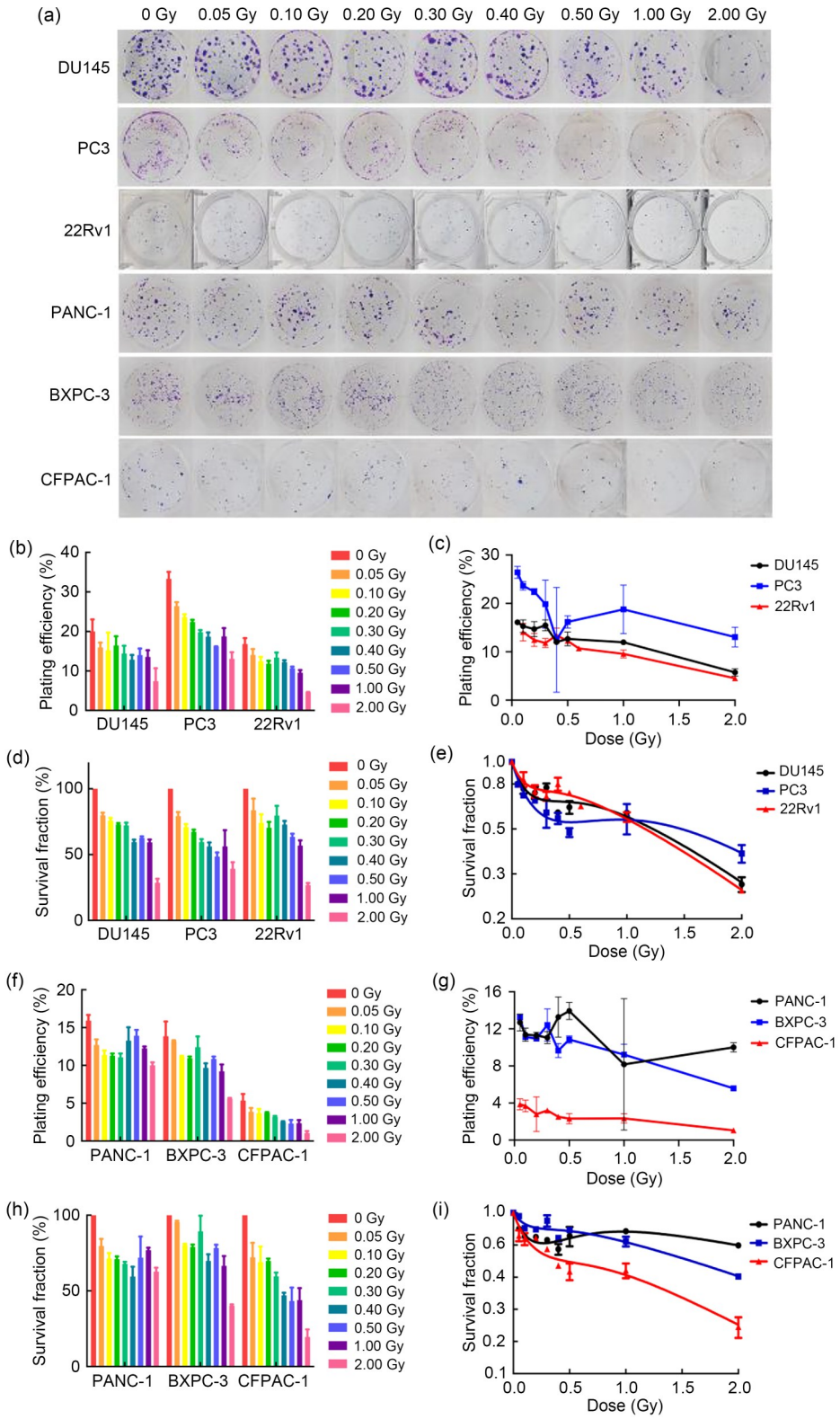

Fig. 2 HRS/IRR phenomenon in human prostate cancer cells and pancreatic cancer cells. (a) The colony formation of human prostate cancer cells and pancreatic cancer cells irradiated with different doses. (b–i) The plating efficiencies, survival fractions, and survival curves of human prostate cancer cells (b–e) and human pancreatic cancer cells (f–i). Values were presented as mean±SD (n=3). HRS: hyper-radiosensitivity; IRR: increased radioresistance; SD: standard deviation.

Table 1 Parameters of HRS/IRR-induced repair model

Cell line	α_r	α_s	d_c (Gy)	β	α/β
DU145	0.4386	3.8260	0.2177	0.0894	4.9060
PC3	0.2610	3.8910	0.3666	0.0953	2.7387
22Rv1	0.4988	3.2410	0.1701	0.0787	6.3380
PANC-1	0.1761	4.6510	0.2357	0.0275	6.4036
BXPC-3	0.3650	2.4200	0.1830	0.0442	8.2579
CFPAC-1	0.7707	4.4800	0.2810	0.0136	56.6691

HRS: hyper-radiosensitivity; IRR: increased radioresistance; α_s: the slope of survival curve of low-dose rate radiation; α_r: the slope of survival curve of high-dose rate radiation; d_c: the threshold of transition from HRS to IRR; β: the indirect lethal effect of radiation on cells; α/β: the radiobiologic ratio of lethal to sublethal damage.

the $t_{1/2}$ of liver and bladder cells. $t_{1/2}$ values of normal pancreas (HPDE6-C7), normal prostate (WPMY-1), and normal rectum (FHC) were calculated by colony formation assay (Fig. 3a) and all normal cell types were irradiated with 2.00 Gy, which was divided evenly into two 1.00 Gy with different intervals at a dose rate of 300 cGy/min. As shown in Fig. 3, when the interval was less than 15 min, the PEs (Figs. 3b–3e) and SFs (Fig. 3f) of normal cells clearly decreased, and subsequently, the survival rate showed a gradually increasing trend with the prolongation of the radiation interval. When the interval was longer than 60 min, radiotherapy did little damage to normal cells, as seen from the latter part of the survival curve, which was almost flat. We defined the location of 50% of sublethal repair on the survival curve as $t_{1/2}$, and the result indicated that the $t_{1/2}$ values of HPDE6-C7, WPMY-1, and FHC cells were 31.2, 22.5, and 40.0 min, respectively. According to the formulae $t=t_{1/2}/(m-1)$, $m=D/d$, the time interval in PLDR of prostate cancer and pancreatic cancer was 3.5 and 2.5 min, respectively. Based

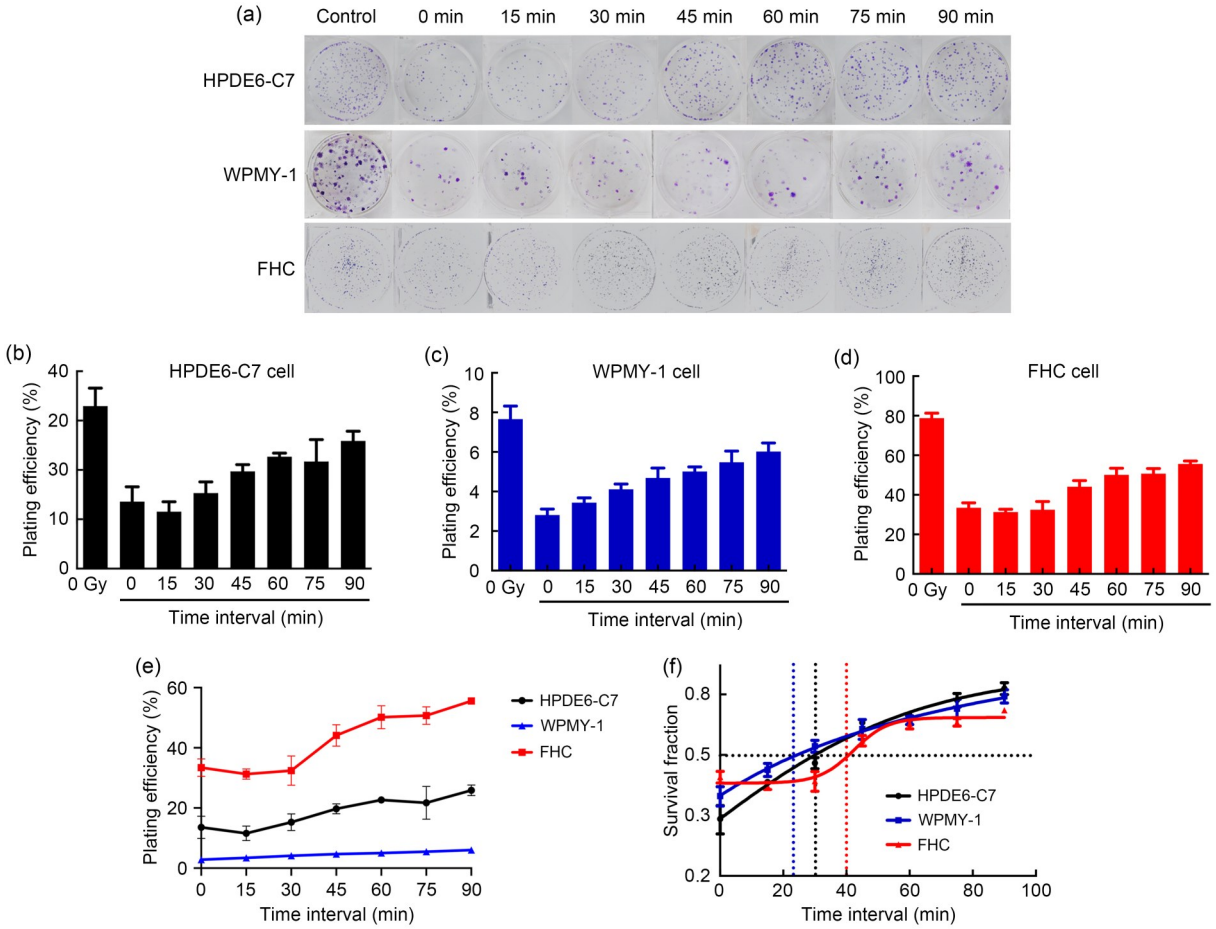

Fig. 3 Sublethal repair half-time ($t_{1/2}$) of human normal cells. (a) The colony formation of human normal cells irradiated with different time intervals; (b–e) The plating efficiencies of human normal pancreatic cells (HPDE6-C7), human normal prostate cells (WPMY-1), and human normal colorectal cells (FHC); (f) The survival curves of human normal cells. Values are presented as mean±SD (n=3). SD: standard deviation.

on the above results, we proposed PLDR strategies for human pancreatic and prostate cancers as follows: (1) human prostate cancer: daily radiation dose 2.00 Gy divided into 10 pulses, interval between two pulses of 2.5 min, and dose rate of 100 cGy/min; (2) human pancreatic cancer: daily radiation dose 2.00 Gy divided into 10 pulses, interval between two pulses of 3.5 min, and dose rate of 100 cGy/min. These two PLDR models were different from the PLDR scheme established by Tome and Howard (2007). This indicated that the dose domain of the HRS phenomenon was different in different tumor tissues, as well as the repair capacity and repair rate of sublethal damage of different normal tissues after radiation. Hence, the establishment of personalized cancer PLDR models may have guiding significance for future clinical treatment.

After determining the PLDR scheme for prostate and pancreatic cancer cells, we compared the effects of PLDR and conventional radiotherapy on the growth of subcutaneous transplanted tumors. Considering that the HRS/IRR phenomena of PC3 cells and PANC-1 cells were more prominent than those of the other cell lines in vitro, we selected PC3 and PANC-1 cells for in vivo experiments. Fifteen male BALB/c nude mice (4–6-weeks old) were injected with PC3 or PANC-1 cells subcutaneously in the distal lower right extremity. When the volume of subcutaneous tumors reached 100–150 mm^3, the mice were randomly divided into three groups (five per group) for different treatments: a control group (no treatment), a conventional radiotherapy group (RT group; 2.00 Gy/d for 3 d at a dose rate of 300 cGy/min), and a PLDR group (treated with the radiotherapy scheme described above). Tumor volumes were measured and calculated every 3 d. Mice were weighed every week. When tumor volumes reached 3000 mm^3 or the surface of the tumor ulcerated, mice were euthanized by carbon dioxide overdose. We obtained tumor growth curves (Figs. 4a and 4d), overall survival curves (Figs. 4b and 4e), and body weight change curves (Figs. 4c and 4f) of tumor-bearing mice. Compared with the control and RT groups, the PLDR group showed significant inhibition of the growth of PC3 and PANC-1 subcutaneous transplanted tumors (PC3: PLDR vs. RT, P=0.045; PANC-1: PLDR vs. RT, P=0.049). With regard to survival time, PLDR significantly prolonged the survival time of PC3 tumor-bearing mice (PLDR vs. control, P=0.0038; PLDR vs. RT, P=0.0045). For PANC-1 mice, although radiotherapy did not extend survival time, surprisingly, PLDR did (PLDR vs. control, P=0.0041). However, it is regrettable that there was no significant difference between the PLDR group and the RT group (PLDR

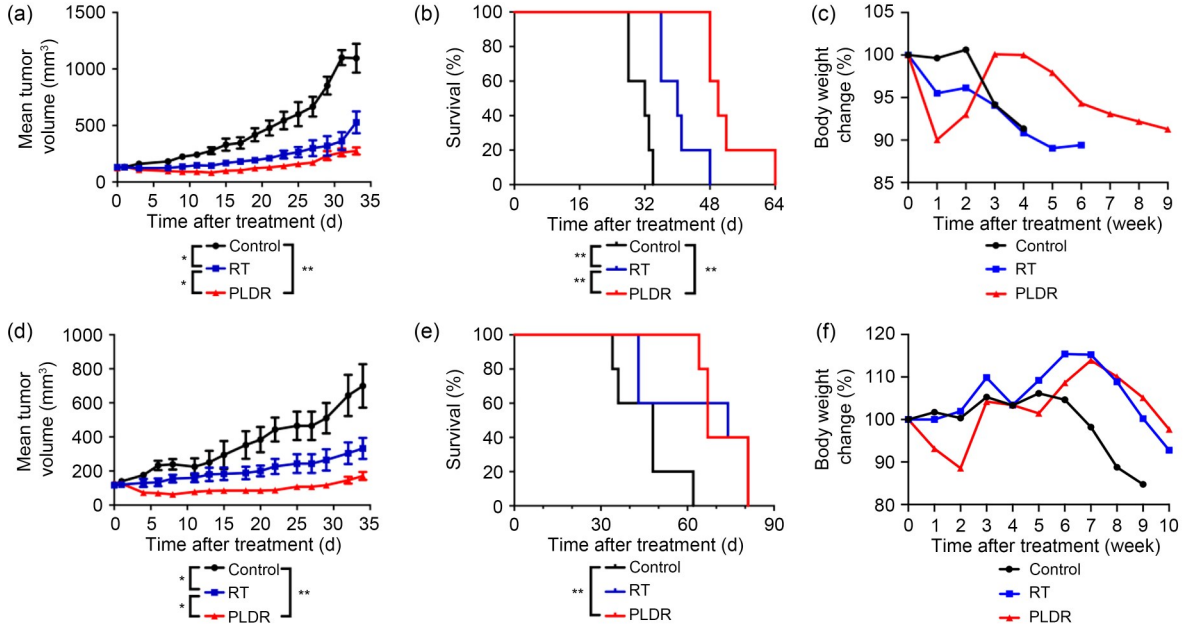

Fig. 4 Effects of PLDR on PC-3 and PANC-1 subcutaneous transplanted tumors. Tumor growth curves (a, d), survival curves (b, e), and body weight change curves (e, f) of mice bearing PC-3-xenograft tumors (a–c) and PANC-1-xenograft tumors (d–f) were generated. Values are presented as mean±SD (n=5). * P<0.05, ** P<0.01. RT: radiotherapy; PLDR: pulsed low-dose rate; SD: standard deviation.

vs. RT, P=0.7455). The results showed that compared with RT, PLDR could significantly inhibit the growth of PC3- and PANC-1-transplanted tumors and prolong the survival of PC3-bearing mice. However, PLDR treatment was not superior to RT in prolonging the survival time of PANC-1-bearing mice, so we conjectured that perhaps PLDR had no advantage in reducing side effects such as weight loss, and that some stress injury response may occur continuously in PANC-1-bearing mice.

Finally, we further investigated whether PLDR inhibited DNA double-strand break (DSB) damage repair and then promoted cancer cell death compared with the traditional radiotherapy schedule (Li and Yuan, 2021). The adherent PC3 and PANC-1 cells seeded in six-well plates were irradiated according to the radiotherapy and PLDR schedules (radiotherapy schedule: both PC3 and PANC-1 cells were irradiated with 6.00 Gy singly at a dose rate of 300 cGy/min; PLDR schedule: PC3 cells were irradiated with 6.00 Gy, which was delivered using 0.20 Gy separated by 2.5 min at a dose rate of 100 cGy/min and PANC-1 cells were irradiated with 6.00 Gy, which was delivered using 0.20 Gy separated by 3.5 min at dose of 100 cGy/min). At different time points after irradiation, cells were harvested for western blot, as in a previous study (Yao et al., 2016). As is well known, phosphorylation of H_2AX at Ser139 (γ-H_2AX) in cell nuclei, which occurs at DSB damage sites, is used as a marker of DNA DSBs (Olive, 2004). Nonhomologous end joining (NHEJ) is one of the main repair methods for DSBs and is mediated by the DNA-dependent protein kinase (DNA-PK), which cannot identify the damage site and requires the helper protein factor KU80 (Zhang and Gong, 2021). Once radiation-induced DSBs form, DNA-PK catalytic subunit (DNA-PKcs) is first recruited to the damaged site, and a KU heterodimer (KU70/KU80) assists the DNA-PK enzyme to recognize the damaged site and participate in DNA damage repair (Blackford and Jackson, 2017). As shown in Figs. 5a, 5e, 5f, and 5j, we found that whether irradiated on traditional radiotherapy or PLDR schedules, PC3 and PANC-1 cells all expressed a higher level of γ-H_2AX as early as 2 h after irradiation (P<0.01). Moreover, PC3 or PANC-1 cells irradiated on the PLDR schedule expressed significantly higher levels of γ-H_2AX than cells irradiated on the radiotherapy schedule (P<0.01). DNA-PKcs expression showed a similar trend 2 h after irradiation (Figs. 5b and 5g). However, 4 h (PANC-1) or 6 h (PC3) after irradiation, the DNA-PKcs and γ-H_2AX expression levels of cells irradiated with PLDR showed no difference from those of non-treated cells, while DNA-PKcs and γ-H_2AX expression levels of cells irradiated with radiotherapy remained relatively high for a long time. At the same time, KU70/KU80 expression in the PLDR group was the same as that in the control group (Figs. 5c, 5d, 5h, and 5i). This indicated that both PLDR and radiotherapy schedules could induce DSBs, but compared with RT, PLDR did not promote effective DNA damage repair. This may explain why cells showed higher radiation sensitivity when irradiated with PLDR than with traditional radiotherapy.

In summary, HRS is a noteworthy phenomenon that plays an important role in traditional radiobiology, and PLDR is an effective re-radiotherapy method. However, most of the research results on the HRS/IRR phenomenon come from studies on isolated cells and animals. The application of HRS/IRR in clinical treatment has just begun, and therefore a large number of clinical studies on PLDR are still needed to provide a stronger theoretical basis and more realistic ideas for clinical treatment of tumors.

Materials and methods

Detailed methods are provided in the electronic supplementary materials of this paper.

Acknowledgments

This work was supported by the Jiangsu Provincial Medical Innovation Team (No. CXTDA2017034), the National Natural Science Foundation of China (No. 81972845), and the Science Foundation of Jiangsu Commission of Health (No. H2018116), China.

Author contributions

Xin WEN performed the experimental research and data analysis, wrote and edited the manuscript. Hui QIU and Zhiying SHAO contributed to the writing and editing of the manuscript. Guihong LIU and Nianli LIU contributed to the study design and experiment guidance. Aoxing CHEN and Xingying ZHANG contributed to the establishment of animal models. Xin DING and Longzhen ZHANG performed the study design, paper guidance, and financial support. All authors have read and approved the final manuscript and, therefore, have full access to all the data in the study and take responsibility for the integrity and security of the data.

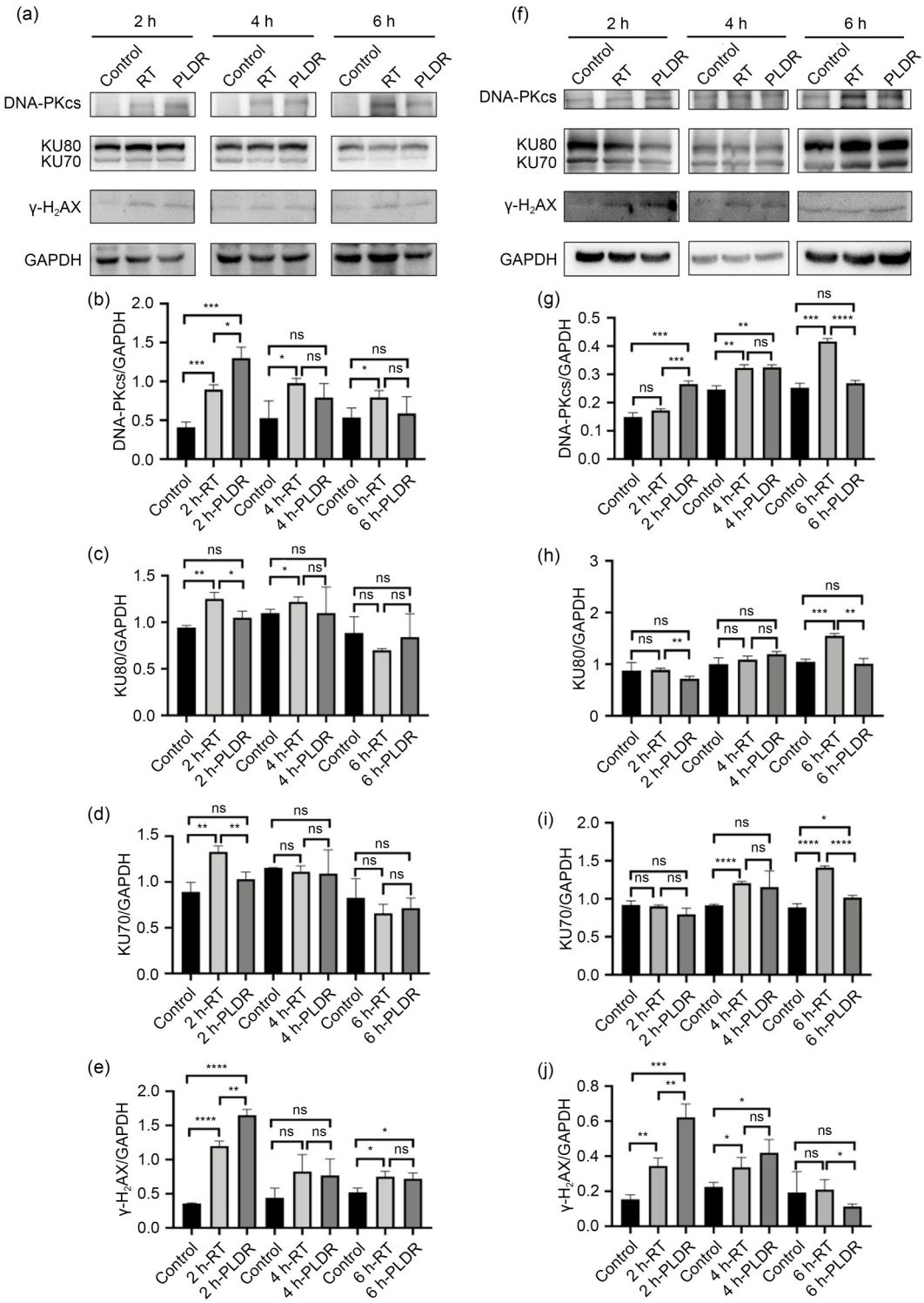

Fig. 5 Effects of RT and PLDR schedules on the expression levels of DNA damage proteins in PANC-1 (a–e) and PC3 (f–j) by western blot. PANC-1 (a) and PC3 (f) cell lysates were collected at different time points for western blot. The band intensities of DNA-PKcs (b, g), KU80 (c, h), KU70 (d, i), and γ-H_2AX (e, j) in PANC-1 (b–e) and PC3 (g–j) cells were quantified after normalized to GAPDH. $^{*}P$<0.05, $^{**}P$<0.01, $^{***}P$<0.001, $^{****}P$<0.0001. Values are presented as mean±SD (n=3). RT: radiotherapy; PLDR: pulsed low-dose rate; DNA-PKcs: DNA-dependent protein kinase catalytic subunit; γ-H_2AX: phosphorylation of H_2AX at Ser139; GAPDH: glyceraldehyde-3-phosphate dehydrogenase; SD: standard deviation; ns: not significant.

Compliance with ethics guidelines

Xin WEN, Hui QIU, Zhiying SHAO, Guihong LIU, Nianli LIU, Aoxing CHEN, Xingying ZHANG, Xin DING, and Longzhen ZHENG declare that they have no conflict of interest.

This article does not contain any studies with human or animal subjects performed by any of the authors.

References

Blackford AN, Jackson SP, 2017. ATM, ATR, and DNA-PK: the trinity at the heart of the DNA damage response. *Mol Cell*, 66(6):801-817. https://doi.org/10.1016/j.molcel.2017.05.015

Combs SE, Schmid TE, Vaupel P, et al., 2016. Stress response leading to resistance in glioblastoma—the need for innovative radiotherapy (iRT) concepts. *Cancers*, 8(1):15. https://doi.org/10.3390/cancers8010015

Dai XF, Tao D, Wu HG, et al., 2009. Low dose hyper-radiosensitivity in human lung cancer cell line A549 and its possible mechanisms. *J Huazhong Univ Sci Technol Med Sci*, 29(1):101-106. https://doi.org/10.1007/s11596-009-0122-4

Elkind MM, Sutton-Gilbert H, Moses WB, et al., 1965. Radiation response of mammalian cells grown in culture. V. Temperature dependence of the repair of X-ray damage in surviving cells (aerobic and hypoxic). *Radiat Res*, 25:359-376. https://doi.org/10.2307/3571978

Harney J, Shah N, Short S, et al., 2004. The evaluation of low dose hyper-radiosensitivity in normal human skin. *Radiother Oncol*, 70(3):319-329. https://doi.org/10.1016/j.radonc.2004.01.015

Li J, Zhao ZH, Du GB, et al., 2019. Safety and efficacy of pulsed low-dose rate radiotherapy for local recurrent esophageal squamous cell carcinoma after radiotherapy: study protocol for a prospective multi-center phase II trial. *Medicine*, 98(26):e16176. https://doi.org/10.1097/MD.0000000000016176

Li Y, Yuan J, 2021. Role of deubiquitinating enzymes in DNA double-strand break repair. *J Zhejiang Univ-Sci B (Biomed & Biotechnol)*, 22(1):63-72. https://doi.org/10.1631/jzus.B2000309

Martin LM, Marples B, Lynch TH, et al., 2013. Exposure to low dose ionising radiation: molecular and clinical consequences. *Cancer Lett*, 338(2):209-218. https://doi.org/10.1016/j.canlet.2013.05.021

Morris DE, 2000. Clinical experience with retreatment for palliation. *Semin Radiat Oncol*, 10(3):210-221. https://doi.org/10.1053/s1053-4296(00)80039-9

Olive PL, 2004. Detection of DNA damage in individual cells by analysis of histone H2AX phosphorylation. *Methods Cell Biol*, 75:355-373. https://doi.org/10.1016/s0091-679x(04)75014-1

Pavlopoulou A, Bagos PG, Koutsandrea V, et al., 2017. Molecular determinants of radiosensitivity in normal and tumor tissue: a bioinformatic approach. *Cancer Lett*, 403:37-47. https://doi.org/10.1016/j.canlet.2017.05.023

Straube C, Scherb H, Gempt J, et al., 2018. Adjuvant stereotactic fractionated radiotherapy to the resection cavity in recurrent glioblastoma—the GlioCave study (NOA 17-ARO 2016/3-DKTK ROG trial). *BMC Cancer*, 18:15. https://doi.org/10.1186/s12885-017-3928-7

Straube C, Kessel KA, Zimmer C, et al., 2019. A second course of radiotherapy in patients with recurrent malignant gliomas: clinical data on re-irradiation, prognostic factors, and usefulness of digital biomarkers. *Curr Treat Options Oncol*, 20(10):71. https://doi.org/10.1007/s11864-019-0673-y

Todorovic V, Prevc A, Zakelj MN, et al., 2020. Pulsed low dose-rate irradiation response in isogenic HNSCC cell lines with different radiosensitivity. *Radiol Oncol*, 54(2):168-179. https://doi.org/10.2478/raon-2020-0015

Tome WA, Howard SP, 2007. On the possible increase in local tumour control probability for gliomas exhibiting low dose hyper-radiosensitivity using a pulsed schedule. *Br J Radiol*, 80(949):32-37. https://doi.org/10.1259/bjr/15764945

Wang Q, Xiao ZY, Lin ZY, et al., 2017. Autophagy influences the low-dose hyper-radiosensitivity of human lung adenocarcinoma cells by regulating MLH1. *Int J Radiat Biol*, 93(6):600-606. https://doi.org/10.1080/09553002.2017.1286052

Yao H, Qiu H, Shao ZY, et al., 2016. Nanoparticle formulation of small DNA molecules, Dbait, improves the sensitivity of hormone-independent prostate cancer to radiotherapy. *Nanomedicine*, 12(8):2261-2271. https://doi.org/10.1016/j.nano.2016.06.010

Zhang F, Gong Z, 2021. Regulation of DNA double-strand break repair pathway choice: a new focus on 53BP1. *J Zhejiang Univ-Sci B (Biomed & Biotechnol)*, 22(1):38-46. https://doi.org/10.1631/jzus.B2000306

Supplementary information

Materials and methods